# LASERLAB-EUROPE

## The Integrated Initiative of European Laser Research Infrastructures III

**Grant Agreement number: 284464**

Work package number 32 – Work package name Innovative radiation sources at the extremes (INREX)

Deliverable number: D32.1

Deliverable name: Report on the implementation of few-cycle to single cycle mid-IR sources

Lead Beneficiary: POLIMI

Due date: Month 36

Date of delivery: Month 37

Project webpage: www.laserlab-europe.eu

| *Deliverable Nature* | |
|---|---|
| R = Report, P = Prototype, D = Demonstrator, O = Other | P |
| *Dissemination Level* | |
| PU = Public<br>PP = Restricted to other programme participants (incl. the Commission Services)<br>RE = Restricted to a group specified by the consortium (incl. the Commission Services)<br>CO = Confidential, only for members of the consortium (incl. the Commission Services) | PU |

**A. Abstract / Executive Summary**

Deliverable 32.1 is related to the implementation of few-cycle to single cycle mid-IR sources. The development of novel sources of high-energy ultrashort light pulses, tunable in the near-mid-infrared can open the way to investigating different fundamental mechanisms from electronic excitation via vibrational motion to off-resonance strong-field effects, such as high harmonic generation (HHG), attosecond streaking or strong-field tunneling ionization.
In this report, the parametric sources developed by POLIMI and ICFO within the work package 32 will be discussed. Ultrashort pulses tunable from 1.2 to 3.1 μm have been generated and characterized, thus enabling ultrafast spectroscopy, and strong field physics in the mid-IR.

**B. Deliverable Report**

## 1 Introduction

Noncollinear optical parametric amplifiers (NOPAs) are used since more than a decade for the generation of tunable femtosecond pulses. Since then, they have been continuously improved to supply high gain over very wide bandwidths within the whole transparency range of the used nonlinear crystals. Their capability of not only preserving the phase of an actively carrier-envelope phase (CEP) stabilized oscillator, but even providing intrinsic, passive CEP stability has only recently moved into focus [1]. In the strong-field regime, the electric field strength rather than the peak or average intensity plays the key role. Thus, for very short pulses, the CEP determines the maximum strength of the electric field and has been demonstrated to be of key importance for coherent control of HHG and attosecond streaking in gases. More recently, similar effects have been demonstrated for photoemission from metallic nanostructures.
Several techniques have been used in the past to produce tunable mid-IR pulses, but they are generally limited to relatively narrowband, multi-cycle pulses of low energy. The objective here is to develop high energy nearly single cycle pulses in the mid-IR, which will allow strong field studies in this spectral region.
POLIMI and ICFO have developed and characterized various sources of few-cycle, passively CEP-stabilized laser pulses tunable between 1.2 and 3.1 μm.

## 2 Objectives

**Objective 1 - ICFO:** Development of two sources for near single-cycle and CEP stable pulses at wavelength of 1.85 nm and 3.1 μm. A specific aspect of both sources is the long term power and CEP stability, making them ideally suited for strong field experiments.

**Objective 2 - POLIMI:** Development of a source of few-cycle, passively CEP-stabilized laser pulses tunable between 1.2 and 2.1 μm for controlling photoemission and motion of electrons by the phase of a strong light field.

## 3 Work performed / results / description

ICFO has developed a mid-IR OPCPA source during the last years, based on an Er:fiber MOPA system which generates mid-IR pulses centered at 3.1 μm via difference frequency generation (DFG). These pulses are passively CEP stabilized to better than 250 mrad rms over 10 min. The system delivers 55 fs (5 optical cycles) pulses at 160 kHz and energy up to 25 microjoules. The overall power stability is better than 1% rms over 44 hours which corresponds to 293 days at 1 kHz. The pulse duration could further be decreased by implementing filamentary self-compression [2]. This results in 7 microjoule pulses at 32 fs or 2.9 optical cycles, as shown in Fig. 1(a). The experimental setup is shown in Fig. 1(b). The stability and utility of this system was very recently demonstrated through recollision electron diffraction to retrieve the bond distances in an aligned acetylene molecule [3].

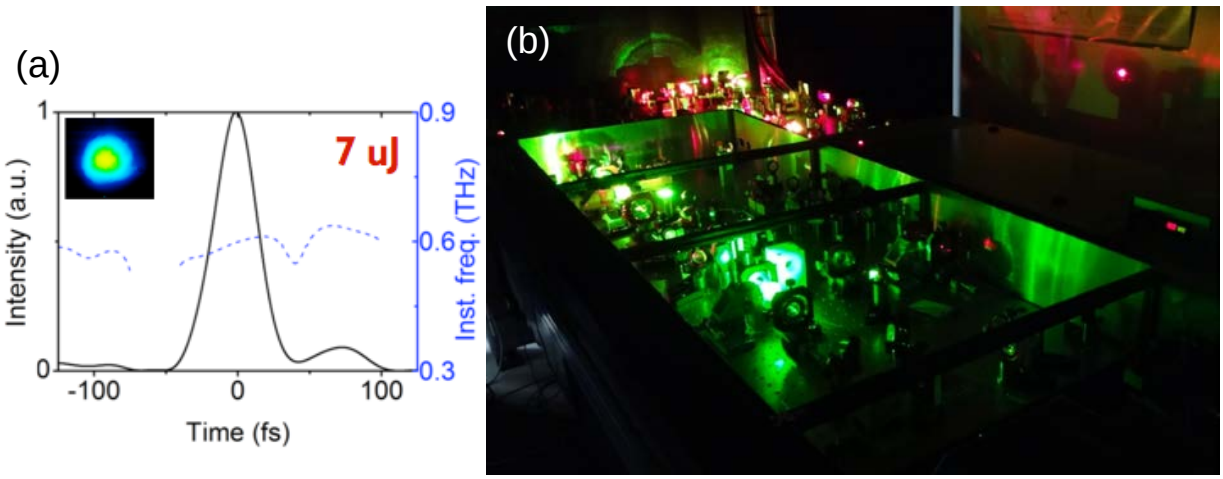


**Fig. 1**: Mid-IR OPCA at 3.1 μm. (a) Measured pulse duration after self-compression in a filament. The inset shows the spatial intensity profile. (b) Photograph of the prototype setup.

The second system is based on a Ti:Sapphire laser system emitting 40 fs pulses at 1 kHz and 10 mJ (a photograph of the prototype setup is shown in Fig. 2). These pulses pump a modified TOPAS OPA system with subsequent hollow fiber compressor. This results in 0.6 millijoule pulses with duration of 10 fs (1.6 optical cycles) at 1.85 μm, as shown in Fig. 3 [4].

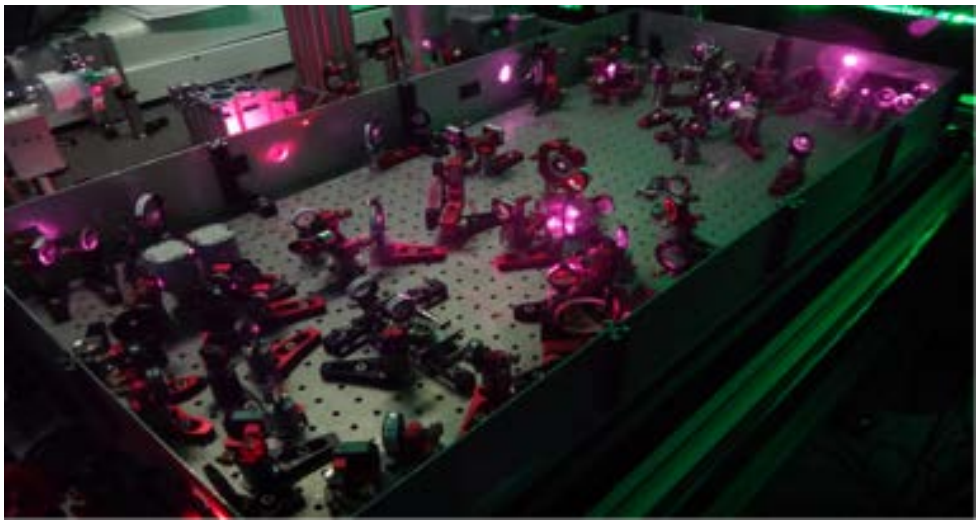

**Fig. 2**: Photograph of the prototype at 1.85 μm.

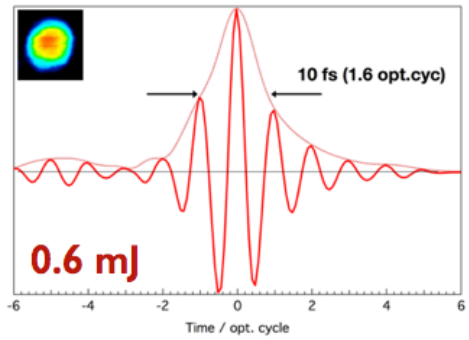


**Fig. 3**: Temporal characterization of the pulses at 1.85 μm at the output of an hollow fiber compressor. The inset shows the spatial intensity profile.

The system is passively CEP stable to better than 90 mrad over 1 hour. Its utility was demonstrated by driving ponderomotively shifted high harmonic generation into and across the water window. This first 1 kHz soft X-ray source was used for a XAFS measurement in condensed matter, demonstrating its applicability for table top XAFS measurements in solid state [3]. Moreover, spatio temporal isolation was implemented and yielded isolated attosecond soft X-ray pulses at the carbon K-shell edge [5].

POLIMI has realized and characterized a source of few-cycle, passively CEP-stabilized laser pulses tunable between 1.2 and 2.1 μm. The approach is based on DFG between the output of two NOPAs, which are seeded by the same white light (WL) and thus share the same CEP. A CEP stability better than 50 mrad was achieved over time spans of seconds up to 20 minutes, when averaging over 100 pulses, which is an excellent long-term CEP stability. The suitability of the CEP-stable laser source for strong-field experiments is demonstrated by measuring the photo-electron yield from a metallic nano-taper as a function of the CEP.

The experimental setup of the ultrafast pulse source is shown schematically in Fig. 4(a). The system can be grouped into two parallel NOPA stages followed by DFG, and it is pumped by a chirped pulse regenerative amplifier system emitting pulses of 120 fs duration at 800 nm center wavelength with a repetition rate of up to 5 kHz and a pulse energy up to 800 μJ. The approach used for this prototype is to generate pulses with a broad bandwidth (and short duration) at a center wavelength around 600 nm in one stage (NOPA#1), and pulses with a narrow bandwidth at 890 nm in the other stage (NOPA#2). With this choice of wavelength for NOPA#2 the spectral properties of NOPA#1 are transferred to the wavelength region around 1.6 μm by DFG between the pulse trains.

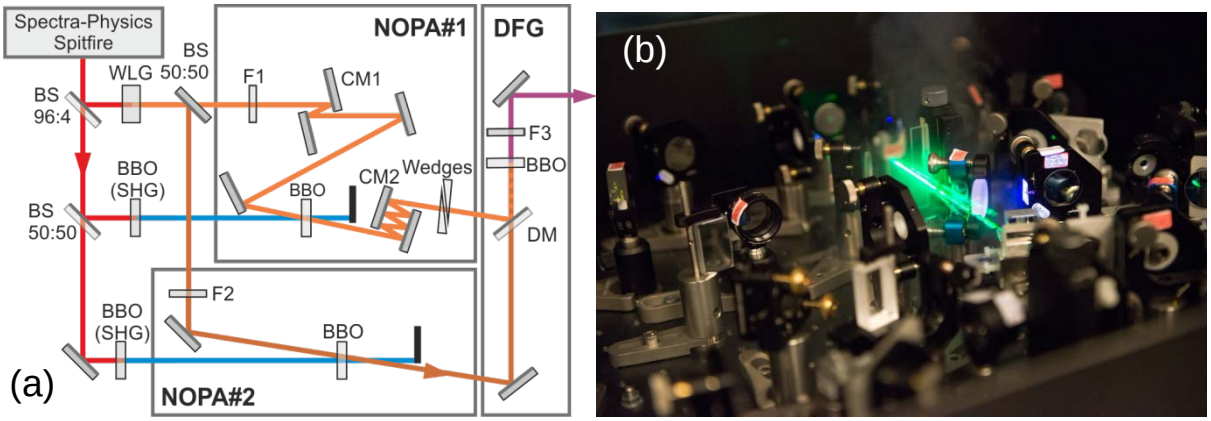


**Fig 4:** (a) Experimental setup. The system is based on pulse generation in two NOPA stages (NOPA#1, NOPA#2), which are seeded by the same white light generation (WLG) source, and subsequent difference frequency generation (DFG) of the two pulse trains. (b) Photograph of the prototype setup.

A small portion of the pump light, with a pulse energy of 600 nJ, is split off and focused into a 2 mm thick sapphire plate to create a WL filament (white light generation, WLG in Fig. 4(a)). The generated WL spans a spectral range from <450 nm to >1 μm. By means of a reflective neutral density filter used as a 50:50 beam splitter (BS), the WL is split into two replicas, which serve as the seed light sources for the two NOPA stages. The major remaining fraction of the available source pulse energy serves as the pump light for the NOPAs. To this aim, the pulse train is split into two pulse trains with an energy of 220 μJ and 260 μJ, respectively, which are frequency-doubled in two 1-mm thick β-barium borate (BBO) crystals cut for type-I

phase matching. This results in two pulse trains at a center wavelength of 400 nm and with pulse energies of 110 μJ and 130 μJ, respectively.
In NOPA#1, the spectral components with wavelengths > 650 nm are suppressed by an absorptive filter, and the chirped WL is partially compressed by one reflection off a pair of chirped mirrors to increase the temporal overlap with the pump pulse and hence broaden the spectrum of the amplified beam. The WL and the 110 μJ second harmonic (SH) pulse train are non-collinearly overlapped in a 1 mm thick BBO crystal cut at an angle of $\theta$ = 32°. In order to support a parametric gain bandwidth in excess of 100 nm, the internal angle between pump and seed is set to 3.7°. The WL is focused using a spherical mirror with 500 mm radius of curvature, and the SH light is focused by a lens of 300 mm focal length. The output of NOPA#1, i.e., the amplified WL, is collimated using a second spherical mirror with 500 mm radius of curvature. The pulses are subsequently compressed by 3 reflections off a second pair of chirped mirrors (CM2) and by transmission through a finely adjusted pair of fused silica wedges.
The seed of NOPA#2 is a fixed narrow-bandwidth pulse, which is extracted from the WL by a bandpass filter of 10 nm bandwidth, centered at 890 nm. This spectral component and the 130 μJ SH pulse trains are non-collinearly overlapped in a 1 mm thick BBO crystal cut at an angle of $\theta$ = 29°. The two pulse trains are focused by two lenses of 250 mm and 300 mm focal length, respectively, and the output of NOPA#2 is collimated using a 250 mm focal length lens.

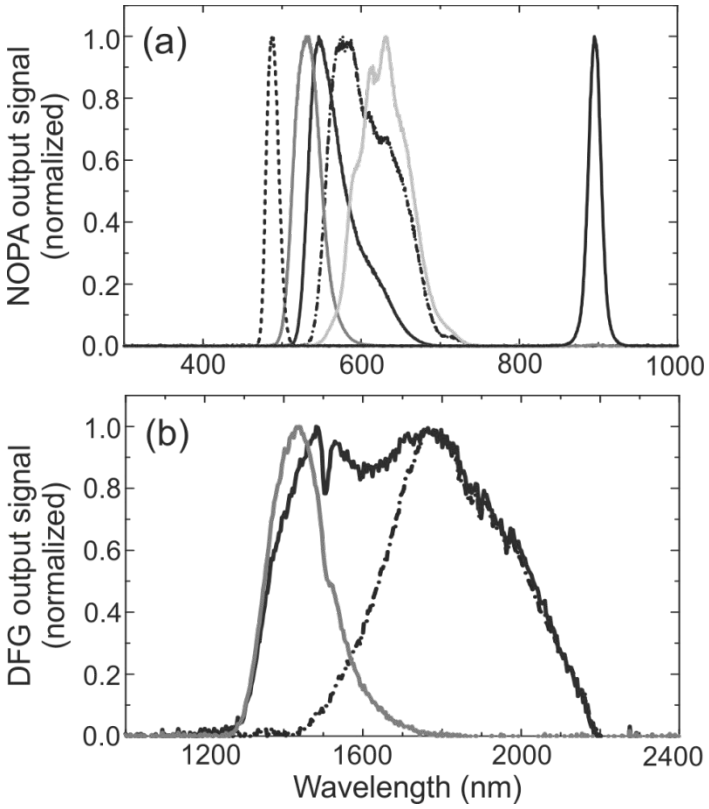


**Fig. 5.** Wavelength tuning of the NOPA-DFG system. (a) Output spectra of the NOPA stages. The spectra at $\lambda$<800 nm are generated by NOPA#1; the wavelength tuning was achieved by changing the time delay between WL and pump pulse. The spectrum at $\lambda$ = 890 nm is the output of NOPA#2. (b) DFG spectra, corresponding to the three center NOPA#1 spectra shown in (a). The detected wavelength range is limited at long wavelengths by the spectral response of the spectrometer.

The output pulse trains of NOPA#1 and NOPA#2 are collinearly combined by a dichroic mirror (DM) and are then focused with a spherical mirror with 200 mm radius of curvature into a 300 μm thick BBO crystal cut at $\theta$ = 32° for type II phase-matched DFG. The generated DFG pulse train is collimated by a second spherical mirror with 200 mm radius of curvature, and the residual input light for the DFG stage is removed by spectral filtering.

By changing the time delay between the WL and the SH pulse train in NOPA#1, the center wavelength of the amplified pulses can be adjusted within the wavelength range between 475 nm and 675 nm [see Fig. 5(a)]. The selected spectral band of the WL seed light is amplified to 5 μJ. The broadest spectrum has a bandwidth of 100 nm centered at 600 nm. The temporal duration of the NOPA#1 pulses is measured using an interferometric frequency-resolved autocorrelation (IFRAC), which yields a near-Fourier limit duration of 7 fs. The second NOPA#2 stage generates pulses with the center wavelength fixed to 890 nm [see black curve in Fig. 5(a)] and with a pulse energy of 2 μJ. After suitable tuning of NOPA#1, the temporal pulse overlap between the two pulse trains in the DFG crystal is adjusted, and the conversion efficiency is optimized by slightly tilting the DFG crystal. With the fixed, narrow-bandwidth output of NOPA#2, the wide bandwidth and tunability of NOPA#1 are directly transferred to the NIR by the DFG process and result in a wavelength coverage from 1350 nm to 2030 nm [see Fig. 5(b)]. Typically a pulse energy of 220 nJ is achieved. The duration of the NIR pulses, measured by IFRAC at a center wavelength of 1.6 μm, is as short as 10.6 fs and corresponds to 2 optical cycles (see Fig. 6(a)).

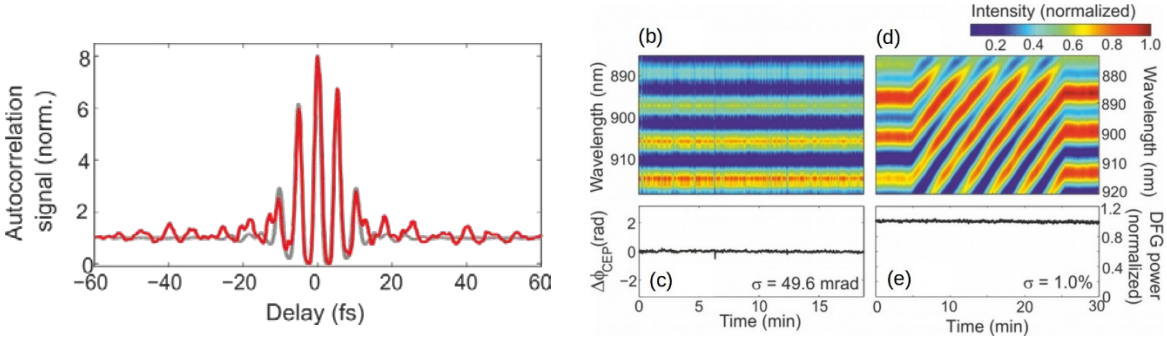


**Fig. 6.** (a) Interferometric autocorrelation trace distilled from an IFRAC measurement of the pulses (red curve), recorded at a center wavelength of 1.6 μm and indicating a pulse duration of 10.6 fs or 2 optical cycles. The grey curve is a simulated autocorrelation trace, calculated from the retrieved electric field strength. (b) Interference fringes measured in the f-to-2f interferometer over a time span of 18 min when averaging over 100 pulses, showing (c) very low residual CEP fluctuations of only 49.6 mrad. (d) By inserting dispersive material, the CEP can be tuned linearly over 10π. (e) shows the power stability of the generated DFG radiation measured over 30 min, with a residual instability of about 1%.

Fluctuations of the CEP are measured in an f-to-2f-interferometer, realized as a common-path interferometer. Fig. 6(b) shows spectral interference fringes recorded behind the f-to-2f interferometer over a period of 18 min. The CEP was extracted from these spectra [Fig. 6(c)], revealing low residual fluctuations of 49 mrad. This compares favorably with a previously reported measurement at a repetition rate of 100 kHz, and is an excellent long-term CEP stability, especially considering that it is achieved in a completely passive manner. By inserting dispersive material in the form of a pair of fused silica wedges, the CEP could be controlled and adjusted over a range of 10π [Fig. 6(d)]. The rms energy stability of the DFG pulses was measured to be < 1% [Fig. 6(e)].

In order to demonstrate the suitability of the presented NOPA-DFG system for the observation of strong-field effects, we illuminated a sharply etched gold nanotaper with the generated NIR, CEP-controlled pulses and recorded electron kinetic energy spectra as a function of the CEP. With the pulse energy adjusted such that photoemission is governed by above-threshold ionization and the onset of strong-field emission, the electron yield is expected to depend strongly on the maximum field strength and thus to vary with the CEP. In this case we observe a variation of electron yield of 50% with CEP. At higher pulse energies, i.e., in the strong-field regime, we expect that the CEP mainly influences the field-driven acceleration of the electrons. This was confirmed by observing a cyclic variation of the cutoff energy of the kinetic energy spectra. Both observations prove that the CEP is sufficiently stable and that the pulse duration is sufficiently short to study the influence of the electric field rather than the envelope on photoemission from single nanostructures. The experiments

on the CEP effect on photoemission from nanostructures in the strong-field regime can be found in [6].

## 4 Conclusions

We have realized OPAs for the generation of few-cycle, passively CEP-stabilized near- and mid-infrared pulses. We believe that the development and handling of such dedicated, ultrashort pulsed laser sources is a key to observe and understand the motion of electron wave packets in solids, e. g. during electronic excitation or charge transfer processes in natural and artificial light harvesting structures.

## 5 References/Publications

[1] C. Manzoni, O. D. Mucke, G. Cirmi, S. Fang, J. Moses, S.-W. Huang, K.-H. Hong, G. Cerullo and F. X. Kartner, “Coherent pulse synthesis: towards sub-cycle optical waveforms”, Laser & Photonics Review **9**, 129-171 (2015). [DOI: 10.1002/lpor.201570020; Laserlab acknowledgement: **yes**; open access: yes]

[2] M. Hemmer, M. Baudisch, A. Thai, A. Couairon, J. Biegert, “Self-compression to sub-3-cycle duration of mid-infrared optical pulses in dielectrics”, Opt. Exp. **21**, 028095 (2013). [DOI: 10.1364/OE.21.028095; Laserlab acknowledgement: **no**; open access: no]

[3] M. Pullen, B. Wolter, A.-T. Lee, M. Baudisch, M. Hemmer, A. Senftleben, C. D. Schröter, J. Ullrich, R. Moshammer, C.-D. Lin, J. Biegert, “Imaging aligned polyatomic molecules with laser-induced electron diffraction”, Nature Commun. **6**, 7262 (2015). [Laserlab acknowledgement: **no**; open access: yes]

[4] S.L. Cousin, F. Silva, S. Teichmann, M. Hemmer, B. Buades, J. Biegert, “High flux table-top soft X-ray source driven by sub-2-cycle, CEP stable, 1.85 µm 1 kHz pulses for carbon K-edge spectroscopy”, Opt. Lett. **39**, 5383 (2014). [DOI: 10.1364/OL.39.005383; Laserlab acknowledgement: **no**; open access: yes]

[5] F. Silva, S. Teichmann, S. L. Cousin, J. Biegert, “Spatio-temporal isolation of attosecond soft X-ray pulses in the water window”, Nature Commun. **6**, 6611 (2015). [DOI: 10.1038/ncomms7611; Laserlab acknowledgement: **yes**; open access: yes]

[6] B. Piglosiewicz, S. Schmidt, D.J. Park, J. Vogelsang, P. Groß, C. Manzoni, P. Farinello, G. Cerullo, and Ch. Lienau, “Carrier-envelope phase effects on the strong-field photoemission of electrons from metallic nanostructures”, Nature Photonics **8**, 37-42 (2014). [DOI: 10.1038/nphoton.2013.288; Laserlab acknowledgement: **yes**; open access: no]